

Cooperative Self-Assembly of Au Atoms and C₆₀ on Au(110) Surfaces

J. K. Gimzewski,* S. Modesti,† and R. R. Schlittler

IBM Research Division, Zurich Research Laboratory, 8803 Rüschlikon, Switzerland

(Received 18 October 1993)

A new cooperative self-assembly process where C₆₀ molecules adsorbed on Au(110)-(1×2) surfaces induce mass transport of Au surface atoms to form a (1×5) interfacial reconstruction is presented. Scanning tunneling microscopy shows that the underlying Au atomic arrangement is modified, maximizing the number of C₆₀ molecules bonded to the Au ridges in a distorted (6×5) hexagonal overlayer.

PACS numbers: 61.16.Ch, 61.46.+w, 68.35.Bs, 87.64.Dz

The availability of macroscopic quantities of C₆₀ has permitted intensive research on the physical and chemical properties of fullerene and C₆₀-based systems [1]. For many technological and scientific applications, understanding and control of the growth mechanism of thin films and the interaction of the first monolayer with the substrate are crucial. Structural investigations of monolayer adsorption of C₆₀ are well suited to the technique of scanning tunneling microscopy (STM) [2-7]. Gold surfaces such as (111) [3,4], (110) [5], and (001) [6] as well as polycrystalline substrates [7] have received particular attention. In all of the reports to date C₆₀ has been shown to exhibit a preference for the formation of a close packed hexagonal overlayer. In the case of Au(111) surfaces, Altman and Colton [4] demonstrated a lifting of the Au reconstruction with the formation of two molecular overlayer domains with close packed directions parallel and rotated by 30° with respect to Au(110). Kuk *et al.* explained their images on Au(100) assuming that the clean (5×20) reconstruction is still present under the C₆₀ layer [6].

In this Letter we present the first observations of a new and thermodynamically stable Au(110) interfacial reconstruction which is induced by C₆₀ adsorption. Clean Au(110) reconstructs into a (1×2) missing row reconstruction in which alternate rows of atoms along [110] are removed to produce stable (111) microfacets with a periodicity of 8.14 Å, some 1.4 Å in height [8]. The (1×2) phase exhibits a highly one dimensional corrugation and therefore presents severe geometric constraints for adsorption. This surface geometry hampers the formation of simple quasihexagonal C₆₀ layers similar to those observed on less textured low index planes [with nearest neighbor (NN) distance close to the bulk value of $a = 10.04$ Å [9]], and consequently serves as a crucial test for the interplay between C₆₀-C₆₀ van der Waals (vdW) interaction and the overlayer-substrate bonding. Au atoms at the ridges of the (111) microfacets with lower coordination compared to the microfacet atoms also serve as a probe for the tendency of the C₆₀ molecules to form chemical bonds.

Our results show that although the geometry of the overlayer is dominated by the C₆₀-C₆₀ interaction, a distorted hexagonal superstructure commensurate with the Au surface is formed. Going beyond this general trend,

the first observations of new superstructures formed by C₆₀ which actually *rearrange the rows of Au atoms into unique reconstruction patterns* are reported. Of the various phases observed, the thermodynamically stable one is found to have the minimum number of nonequivalent adsorption sites, where C₆₀ sits in close proximity to an Au ridge atom. Tunneling spectroscopy indicates that a significant fraction of the lowest unoccupied molecular orbitals (LUMO) of C₆₀ broadens and shifts/splits downwards towards the Fermi level. Both of these observations show that the substrate C₆₀ interaction is not simply vdW and that covalent or ionic bonding plays a significant role in a *cooperative self-assembly process*.

The Au(110) surface used in this study was prepared by cycles of Ne⁺ sputtering and annealing at 700 K. The cleanliness of the Au substrate was checked by x-ray photoelectron spectroscopy (XPS). The STM used in this study is a room temperature version of a low-temperature STM [10]. The clean Au(110) surfaces display the typical (1×2) "missing row" reconstruction, interspread by steps over the entire surface, as reported elsewhere [8]. C₆₀ molecules (purity 99.99%) were dosed on this surface at 300 K from a well outgassed W crucible heated at 760 K at a pressure of 1×10^{-11} Pa. No contamination signal other than C was detected by XPS on the Au sample after the dosing. Details of sample and tip preparation are reported in Ref. [8].

STM images show that at low coverages C₆₀ adsorbs at [001] oriented kinks of the [110] steps forming small 2D islands with short-range hexagonal geometry and no superstructure. After adsorption at room temperature some (1×3) missing row troughs appear in the Au(110)-(1×2) terraces. At saturated monolayer coverage these Au terraces are covered with small hexagonal C₆₀ domains exhibiting orientational disorder, as shown in Fig. 1(a). This room temperature disordered phase was found to be metastable. After annealing at 700 K and cooling back to 300 K at coverages less than a saturated monolayer, or after dosing at $T > 600$ K, a new highly ordered phase, shown in Fig. 1(b), is obtained. It is formed by large 2D ordered islands of C₆₀ several hundred Å wide with quasihexagonal coordination and a 2×3 "zigzag" superstructure (with respect to the simple hexagonal C₆₀ lattice). The zigzag lines (bright is higher, dark is lower) run parallel to the [110] gold rows and are verti-

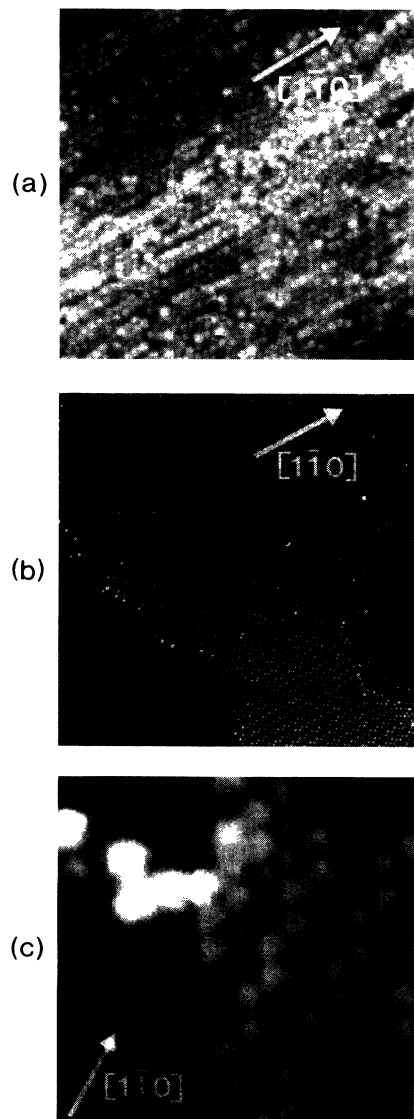


FIG. 1. Topographs of (a) disordered C_{60} monolayers dosed at 300 K on Au(110) ($420 \times 420 \text{ \AA}^2$); (b) after annealing at 700 K ($850 \times 850 \text{ \AA}^2$); (c) (1×5) reconstruction of the Au(110) surface (left corner of the image) close to the edge of a 21 \AA phase C_{60} island.

cally displaced by about 1 \AA . We refer to this structure as the “ 21 \AA phase.” The separation between the brighter molecules in $[001]$ is $21.0 \pm 0.5 \text{ \AA}$. Topographic images of the 21 \AA phase were found to be independent of tip polarity and voltage V_t within $2000 \text{ mV} > |V_t| > 5 \text{ mV}$.

The formation of the well-ordered 21 \AA phase occurs by thermal activation only at C_{60} coverages less than a saturated monolayer. Complete C_{60} monolayers dosed at 300 K and annealed at 700 K show only small patches with the 21 \AA phase of Fig. 1(b) coexisting with regions without superstructures and with regions where the hexagonal C_{60} lattice is modulated by two other superstruc-

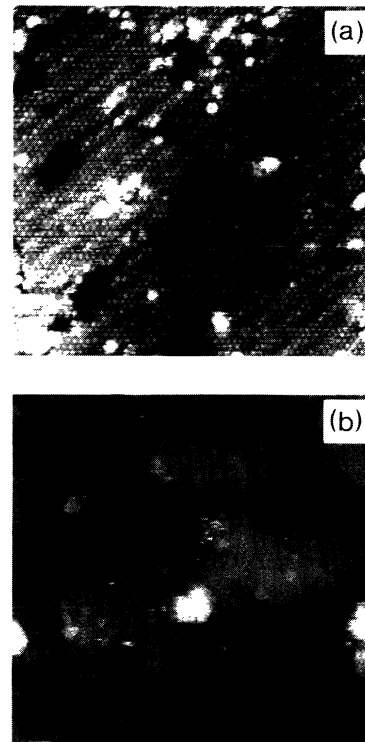


FIG. 2. Topographs of (a) second C_{60} layer dosed on top of a (6×5) 21 \AA phase C_{60} monolayer at 300 K; and (b) third layer of C_{60} .

tures. One of these is formed by 180° out-of-phase zig-zag rows of molecules $\sim 1 \text{ \AA}$ lower than the others, running parallel to the $[1\bar{1}0]$ direction and spaced by $26.0 \pm 0.5 \text{ \AA}$. Another is formed by linear chains of C_{60} molecules rising by $\sim 1 \text{ \AA}$ with respect to the others and tilted by $\sim 54^\circ$ away from $[1\bar{1}0]$ with a separation of $27.5 \pm 0.5 \text{ \AA}$. In this phase the plane of the C_{60} layer is tilted by $\sim 2^\circ$ with respect to that of the other superstructure in the direction normal to the lines. At higher C_{60} doses on top of a 21 \AA phase, the growth of the film was found to occur in a *layer-by-layer mode*. The second layer [Fig. 2(a)] shows long-range order and a small residual corrugation with a 21 \AA period arising from that of the first layer, while the third layer [Fig. 2(b)] is essentially flat. From these observations we conclude that the interfacial 21 \AA phase remains stable even when a second layer is deposited.

The electronic structure of the first C_{60} monolayer is appreciably affected by adsorption as evidenced by tunneling spectroscopy of the first and second layer C_{60} molecules. First, half a monolayer of C_{60} was sublimed onto Au followed by annealing and sequences of i/v curves were recorded placing the tip of the STM alternatively on the bare Au surface and on the C_{60} islands. Then the coverage was increased up to 1.5 monolayers followed by annealing and further i/v curves were recorded alternatively on the first and the second C_{60} layers. This pro-

cedure minimizes interpretational problems associated with the electronic structure of the tip. The normalized spectra, $d[\ln(i/v)/dv]$ are shown in Fig. 3 for clean Au, first layer C_{60} , and second layer C_{60} . From the spectra we conclude that the C_{60} molecules in the second layer are semiconductorlike with an estimated gap of ~ 2.0 eV between the highest occupied molecular orbital (HOMO) (centered 1.4 eV below E_F) and the LUMO peaks (1.4 eV above E_F), in good agreement with the gap measured by direct and inverse photoemission in solid C_{60} [11]. The density of states of clean Au is metalliclike, i.e., flat across the Fermi level, whereas C_{60} molecules in the first layer exhibit a peak at ~ 1.5 eV below the Fermi level, corresponding to the HOMO structure for the second layer. In comparison the LUMO derived structure broadens, shifts down in energy, and reaches the Fermi level.

The structural and electronic characteristics of the 21 Å phase at the C_{60} -Au(110) interface can be consistently explained in terms of a strong adsorbate-substrate interaction. The 21 Å spacing, which is not commensurate to that of the (1×2) rows (8.16 Å), points to a Au reconstruction at the C_{60} -Au interface induced by the molecule-substrate interaction. A new Au reconstruction with a periodicity which explains the island superstructure was found also on some regions of the bare Au(110) terraces after C_{60} adsorption and is shown in Fig. 1(c). It is a 1×5 structure formed by alternating (1×2) and (1×3) rows with a lattice parameter of 20.5 Å in $[001]$, in good agreement with the periodicity of the C_{60} zigzag superstructure. We used a simple hard sphere model based on the (1×5) reconstruction to model the geometry of the C_{60} superstructure (Fig. 4). The light-colored balls representing C_{60} molecules [Figs. 4(a)–4(c)] lying close to

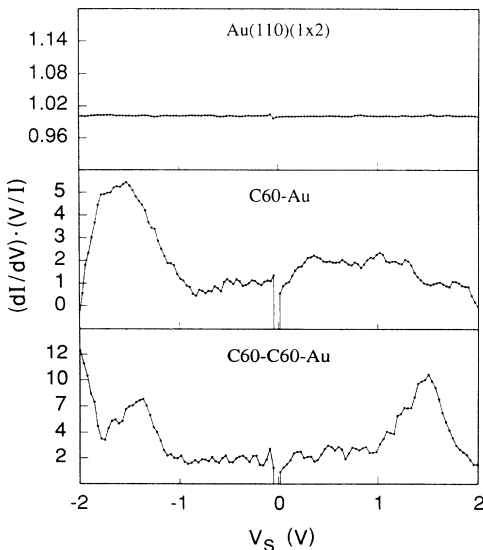


FIG. 3. Tunneling spectra of Au(110) (1×2) and the first and second monolayers of C_{60} on Au(110).

the Au (1×3) ridges are ~ 1 Å higher than the darker balls in close proximity to the (1×2) ridges and agree well with the structure of the STM topograph. A model of the unit cell of one C_{60} overlayer (open circles) is shown with respect to underlying Au reconstruction in Fig. 4(c). The significant Au mass transport required to switch from the (1×2) to the (1×5) missing row reconstruction explains why the stable configuration is reached only after high-temperature annealing. Low energy electron diffraction (LEED) on the 21 Å phase shows clear extra diffraction spots in a position $(n/6, m/5)$ compatible with a (6×5) unit cell, commensurate with the substrate in the $[1\bar{1}0]$ direction, where the surface primitive vector corresponds to 6 times that of the Au substrate. The other 26 Å and 27 Å period phases can be similarly explained by C_{60} adsorption on (1×6) reconstructed (110) terraces and on periodically stepped (1×2) reconstructed (110) terraces [12], respectively. These two phases do not develop after annealing if the C_{60} coverage is less than a saturated monolayer. Consequently, the (1×6) and the stepped (1×2) phases are metastable and form only because a complete coverage of the Au surface by C_{60} molecules severely limits the Au atom mobility.

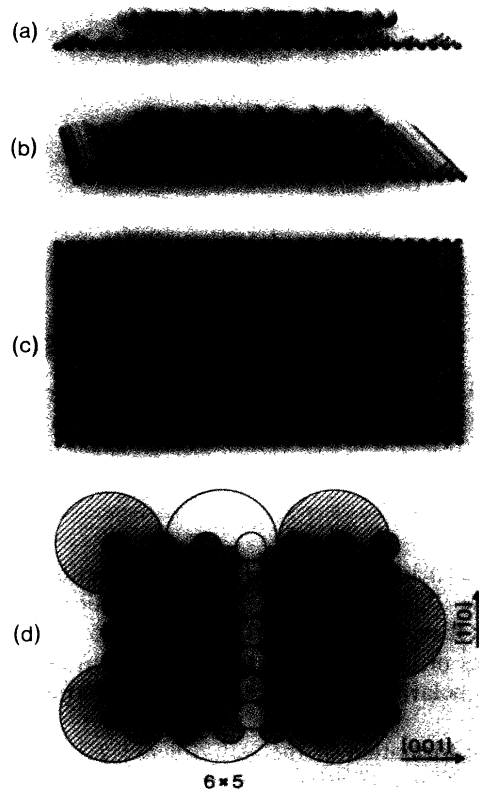


FIG. 4. Hard sphere model for the (6×5) zigzag structure of 1 C_{60} ML on Au(110). (a) Side view, (b) perspective view, (c) top view, (d) unit cell. (See text for details.) Note that (a)–(c) show the C_{60} cage diameter, whereas in (d) the van der Waals diameter is shown.

We now discuss *why the Au reconstruction changes after C₆₀ adsorption and why (6×5) is the preferred structure*: If the Au substrate maintains its (1×2) reconstruction and a quasihexagonal C₆₀ overlayer is placed on top of it, a commensurate structure is obtained only if the C₆₀-C₆₀ distance is contracted or expanded by about 5% with respect to the bulk equilibrium value, or if the unit cell is very large. In this case several inequivalent adsorption sites are occupied. Commensurability with a close packed structure, a relatively small unit cell and only two adsorption sites can, however, be maintained if a periodic sequence of Au steps are introduced [12]. The model for the (6×5) phase shows that the C₆₀-C₆₀ distances are different from the bulk value by less than 1.5% (10.04 and 10.2 Å) and that only two almost equivalent adsorption sites are present, i.e., on top of Au atoms at the ridge of the (1×2) rows and on top of those at the ridge of the (1×3) rows. These ridge atoms have only seven Au NNs, while other surface atoms have nine NNs. Therefore in the (6×5) structure all the molecules are in close proximity to the more chemically active Au atoms. The estimated energy difference between (1×2), (1×3), and (1×4) Au(110) reconstructions is $\sim 2 \text{ meV } \text{Å}^{-2}$ [13]. Consequently, binding energy (BE) difference between nonequivalent adsorption necessary to balance the reconstruction cost should be $\sim 0.2 \text{ eV}$ per molecule. Purely vdW Au(110)-C₆₀ interaction is hardly compatible with such a value, which is a large fraction of the expected vdW BE and would favor adsorption on the (111) microfacets, since the vdW BE is additive. Ionic bonding is not expected to be important on flat surfaces, because the work function of Au(110) is about 5.3 eV [14], while the BE increase of an adsorbed C₆₀ molecule after a one electron transfer is estimated to be only 3.6 eV [15]. However, the BE of C₆₀ could be substantially higher if it sits on top of an Au ridge and chemical bonds are established [15]. Therefore, the strong tendency towards binding to top Au atoms indicates either substantial covalent site-specific bonding or ionic bonding, i.e., charge transfer. This picture is supported also by tunneling spectroscopy which shows that the energy tail of the LUMO derived structure crosses the Fermi level. The presence of a significant density of states at the Fermi level appreciably modifies the line shape of the C 1s core level photoemission peak through better screening and the Doniac-Sunjic mechanism. The BE of the XPS C 1s peak of the first C₆₀ layer decreases by 0.5 eV and is markedly more asymmetric than that of a multilayer, with a clear tail on the high-BE side, and the linewidth increases by $\sim 0.3 \text{ eV}$ [12], similar to that measured on Cu(110) [16]. The first

(6×5) C₆₀ layers contain only molecules with two very similar adsorption sites whose C 1s BE difference cannot be more than 0.1 eV (the difference in the C 1s BE shifts of C₆₀ on different metals [17]). We attribute most of the increased asymmetry of the C 1s line shape to electron-hole excitation within the LUMO derived states.

In conclusion, we have presented experimental evidence for a new missing row reconstruction formed by a cooperative self-assembly process at the interface between Au(110) and C₆₀. Its structure derives from the balance between the C₆₀-C₆₀ vdW interaction which favors the formation of simple hexagonal C₆₀ layers and the strong C₆₀-Au interaction which favors bonding to the topmost Au atoms of the [110] rows. The significant Au mass transport required is favored by the high mobility of the Au surface atoms and by the small energy difference between the (1×2) and (1×3) Au missing row reconstructions.

We thank B. Reihl for discussions, H. Rohrer and P. Guéret for support, B. Whetton for providing the C₆₀ samples, and E. P. Stoll for assistance with computer modeling.

*To whom correspondence should be addressed. Electronic address: gim@zurich.ibm.com

†Visiting professor from TASC Laboratory, Padriciano 99, 34012 Trieste, Italy.

- [1] See, for instance, *The Fullerenes*, edited by H. W. Kroto, J. E. Fischer, and D. Cox (Pergamon, Oxford, 1993).
- [2] See, for instance, Y. Z. Li *et al.*, *Science* **252**, 547 (1991); **253**, 429 (1991); *Phys. Rev. B* **45**, 13837 (1992).
- [3] R. J. Wilson *et al.*, *Nature (London)* **348**, 621 (1990).
- [4] E. J. Altman and R. J. Colton, *Surf. Sci.* **279**, 49 (1992).
- [5] Y. Zhang, X. Gao, and M. J. Weaver, *J. Phys. Chem.* **96**, 510 (1992).
- [6] Y. Kuk *et al.*, *Phys. Rev. Lett.* **70**, 1948 (1993).
- [7] J. L. Wragg *et al.*, *Nature (London)* **348**, 623 (1990).
- [8] J. K. Gimzewski, R. Berndt, and R. R. Schlittler, *Phys. Rev. B* **45**, 6844 (1992), and references therein.
- [9] P. A. Heiney *et al.*, *Phys. Rev. Lett.* **66**, 2911 (1991).
- [10] R. Gaisch *et al.*, *Ultramicroscopy* **42-44**, 1621 (1992).
- [11] R. W. Lof *et al.*, *Phys. Rev. Lett.* **68**, 3942 (1992).
- [12] J. K. Gimzewski, S. Modesti, and R. R. Schlittler (unpublished).
- [13] F. Ercolessi, M. Parrinello, and E. Tosatti, *Philos. Mag. A* **58**, 213 (1988).
- [14] H. B. Michaelson, *J. Appl. Phys.* **48**, 4729 (1977).
- [15] E. Burnstein *et al.*, *Phys. Scr.* **T42**, 207 (1992).
- [16] J. E. Rowe *et al.*, *Int. J. Mod. Phys. B* **6**, 3909 (1992).
- [17] T. R. Ohno *et al.*, *Phys. Rev. B* **44**, 13747 (1991); S. J. Chase *et al.*, *Phys. Rev. B* **46**, 7879 (1992).

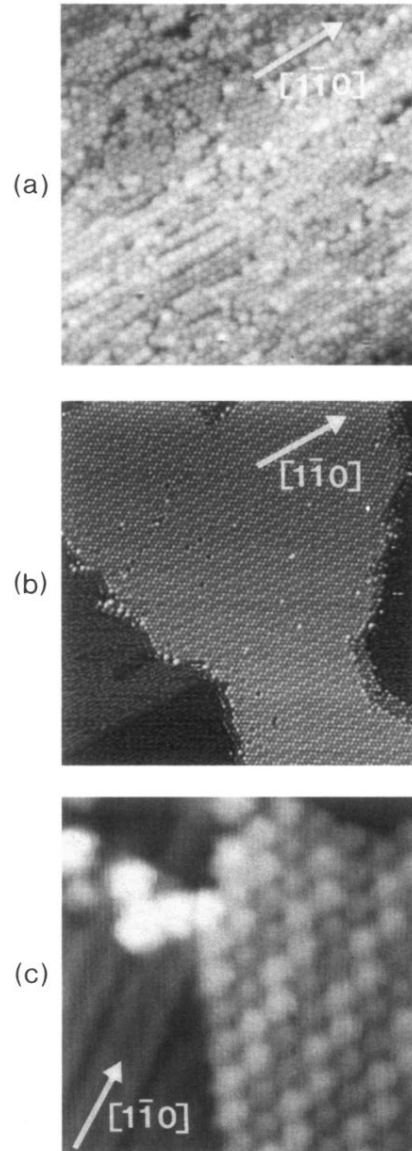


FIG. 1. Topographs of (a) disordered C₆₀ monolayers dosed at 300 K on Au(110) (420×420 Å²); (b) after annealing at 700 K (850×850 Å²); (c) (1×5) reconstruction of the Au(110) surface (left corner of the image) close to the edge of a 21 Å phase C₆₀ island.

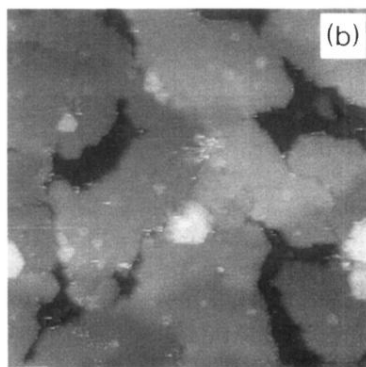
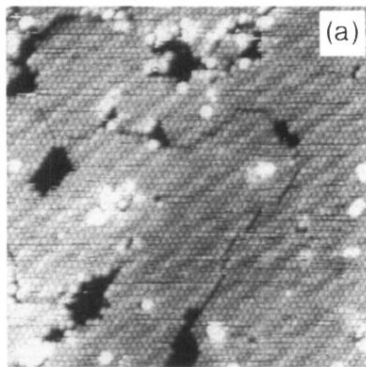


FIG. 2. Topographs of (a) second C_{60} layer dosed on top of a (6×5) 21 \AA phase C_{60} monolayer at 300 K; and (b) third layer of C_{60} .

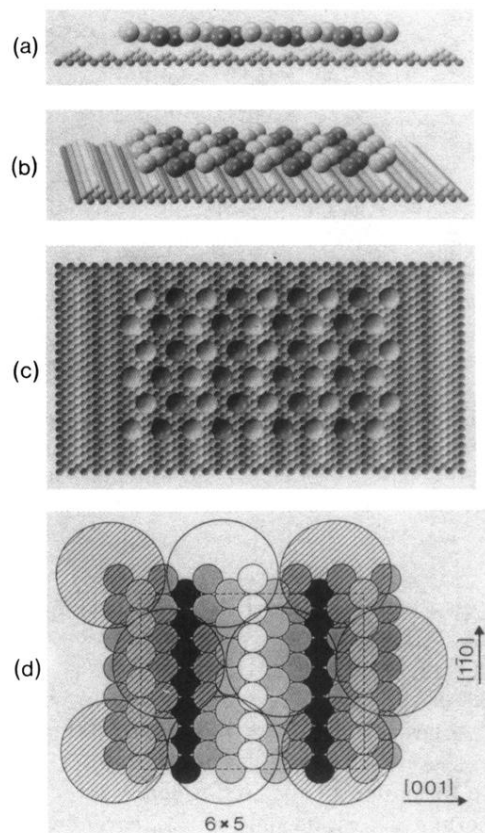


FIG. 4. Hard sphere model for the (6×5) zigzag structure of 1 C_{60} ML on Au(110). (a) Side view, (b) perspective view, (c) top view, (d) unit cell. (See text for details.) Note that (a)–(c) show the C_{60} cage diameter, whereas in (d) the van der Waals diameter is shown.